

See discussions, stats, and author profiles for this publication at: <https://www.researchgate.net/publication/267101704>

# DNAzyme-Based Plasmonic Nanomachine for Ultrasensitive SERS Detection of Lead Ions via a Particle-on-a-Film Hot Spot Construction.

ARTICLE in ANALYTICAL CHEMISTRY · OCTOBER 2014

Impact Factor: 5.64 · DOI: 10.1021/ac5038736 · Source: PubMed

CITATIONS

2

READS

44

7 AUTHORS, INCLUDING:



**Cuicui Fu**

Jilin University

9 PUBLICATIONS 18 CITATIONS

SEE PROFILE



**Hailong Wang**

Jilin University

18 PUBLICATIONS 36 CITATIONS

SEE PROFILE



**Lijia Liang**

Jilin University

5 PUBLICATIONS 15 CITATIONS

SEE PROFILE



**Shuping Xu**

Jilin University

101 PUBLICATIONS 1,371 CITATIONS

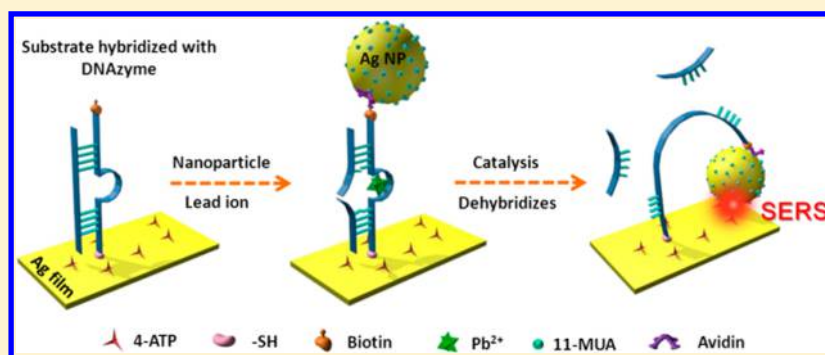
SEE PROFILE

# DNAzyme-Based Plasmonic Nanomachine for Ultrasensitive Selective Surface-Enhanced Raman Scattering Detection of Lead Ions via a Particle-on-a-Film Hot Spot Construction

Cuicui Fu, Weiqing Xu, Hailong Wang, Han Ding, Lijia Liang, Ming Cong, and Shuping Xu\*

State Key Laboratory of Supramolecular Structure and Materials, Institute of Theoretical Chemistry, Jilin University, 2699 Qianjin Avenue, Changchun 130012, P. R. China

## S Supporting Information



**ABSTRACT:** We propose a highly sensitive and selective surface-enhanced Raman scattering (SERS) method for determining lead ions based on a DNAzyme-linked plasmonic nanomachine. A metallic nanoparticle-on-a-film structure was built through a rigid double-stranded bridge linker composed of a DNAzyme and its substrate. This DNAzyme could be activated by lead ions and catalyze a fracture action of the substrate. Thus, the double chain structure of DNA would turn into a flexible single strand, making the metal nanoparticles that connected to the terminal of DNAzyme fall to the surface of the metal film. Hereby, a narrow gap close to 2 nm generated between metal nanoparticles and the metal film, exhibiting a similar effect of a “hot spot” and remarkably enhancing the signal of randomly dispersed Raman-active molecules on the surface of metal film. By measuring the improvement of SERS intensity of the Raman-active molecules, we realized the lowest detection concentration of  $\text{Pb}^{2+}$  ions to 1.0 nM. This SERS analytical method is highly selective and can be extended universally to other targets via the accurate programming of corresponding DNA sequences.

Lead ions do extreme harm to human health and children's intelligence. In the human body, if the amount of lead reaches 10 mg per deciliter in blood, or more than 0.08 mg per liter in urine, it can be identified as the “lead poisoning.” In order to prevent lead poisoning, scientists are constantly exploring the methods for highly sensitive and selective detection of lead ions.<sup>1,2</sup>

As an effective analytical tool, surface-enhanced Raman scattering (SERS) spectroscopy has been widely used for the detection of heavy metal ions due to its ultrahigh sensitivity from million-times enhancement of Raman signal.<sup>3,4</sup> There are mainly two mechanisms contributing to SERS signal: chemical enhancement and physical enhancement,<sup>5,6</sup> wherein the electromagnetic (EM) enhancement effect is the main reason for the SERS phenomenon.<sup>5</sup> The most important “hot spot” model in the EM theory has attracted great attention.<sup>7,8</sup> When two metal nanoparticles (NPs) approach each other,<sup>9</sup> or a metal tip accesses to a metal surface,<sup>10</sup> or a metal NP is laid above a metal film,<sup>11,12</sup> there will be an ultrahigh localized EM field generated at the nanosized gap, where the SERS signal of probed molecules located in this EM field will be improved

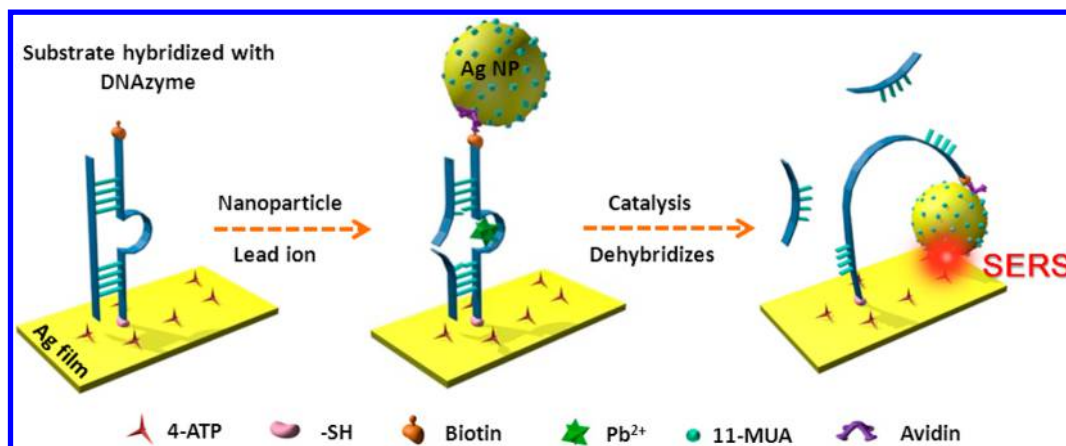
$10^{14}$ – $10^{15}$  times. The enhancement is so huge that single-molecule detection can be realized.<sup>13–15</sup> The formation of a “hot spot” is strictly relevant to the size of the gap,<sup>16–18</sup> and tiny changes in nanoscale will bring a remarkable difference in the enhancement of SERS. In addition, another crucial aspect is that the probed molecules are required to be exactly laid in the gaps, which can ensure the right and high response of the probed matters.

Biological molecules with bioidentification functions, such as, antigen/antibody, biotin/avidin, DNA, enzyme/substrate, and so on, were often employed to fabricate the sandwich structure as bridging molecules for the purpose of the development of novel bioassays.<sup>19–22</sup> Among them, the aptamer becomes one of most favorable objects due to its unique advantages, such as tunable sequences for programming functions, reversible hybridization for dynamic switches, and adjustable flexibility for the designs of nanomachines, etc.<sup>23</sup> On the basis of these

Received: August 20, 2014

Accepted: October 19, 2014

Scheme 1. Schematic Diagram of the Fabrication of the DNAzyme-Based Plasmonic Nanomechine and Its Mechanism for the Detection of  $\text{Pb}^{2+}$



characteristics, aptamer is extremely useful in the fields of biological/chemical sensing. Since the vast majority of DNAzymes require divalent cations as cofactors, the DNAzyme is one of the most specific biosensors for metal ions.<sup>24–26</sup> For example, Wang and Irudayaraj developed a “signal off” SERS strategy for  $\text{Pb}^{2+}$  ion determination via a DNAzyme-based catalytic reaction, in which the Au NPs conjugated DNAzyme will be cleaved from the gold surface upon binding of  $\text{Pb}^{2+}$  ions and decrease SERS intensity.<sup>24</sup>

Here, we report a DNAzyme-based SERS sensing method for lead ion detection. It is a “signal on” strategy based on a mechanical switch occurring on an Ag NP-on-an-Ag film structure, in order to achieve a nanogap with strong localized EM field similar to a “hot spot”. This design insures a highly sensitivity and selectivity for lead ion tracing.

The lead ion nanosensor that we designed in present study is shown in Scheme 1. It is an Ag NP-on-an-Ag film structure on a smooth glass slide with DNAzyme and its substrate DNA as a spacer. A DNAzyme sequence containing 36 bases was applied, which can specifically recognize lead ions.<sup>27–29</sup> A thiol group and a biotin-TEG were conjugated to the 5' and 3' ends, respectively (see the Supporting Information). Then, the substrate (a complementary DNA chain consisting of 21 bases) was hybridized with the above DNAzyme to form a double strand (ds-DNA), which is confirmed by X-ray photoelectron spectroscopic results in the Supporting Information. In the presence of  $\text{Pb}^{2+}$  ions, the DNAzyme would be activated to catalyze a cracked behavior of its substrate strand and then a flexible single-stranded DNA chain would form.<sup>27–29</sup> The Ag NP linked to this DNA chain would drop down to the Ag film, forming a very narrow gap with the spacers involving the surfactants (11-mercaptopundecanoic acid, 11-MUA) on the surface of the Ag NP and the Raman-active molecules (4-aminothiophenol, 4-ATP) previously laid on the Ag film. Similar to a “hot spot” configuration, the localized EM field at the gap would become extremely strong and the SERS signal of 4-ATP would be greatly enhanced. Therefore, we achieved a highly sensitive detection of  $\text{Pb}^{2+}$  ions by the design of a DNAzyme-based plasmonic nanomechine.

To characterize the configuration of the Ag NP-on-an-Ag film structure, we employed the Rayleigh scattering of metal NPs under a dark-field microscope to prove the achievement of DNA and Ag NP assemblies and the response of DNAzyme for  $\text{Pb}^{2+}$  ions. Individual metal NP have strong Rayleigh scattering

and the colors of scattering light depend on the spectral profile of resonance wavelengths.<sup>30</sup> Many factors can affect the scattering of metal NPs, including the particle size, shape, and the refractive index of surrounding.<sup>31</sup> When a metal NP-on-a-metal film structure is illuminated under dark-field illumination, the scattering peak of a metal NP shows a red shift with the distance of the metal NP against the metal film decreasing due to the appearance of strong EM coupling between the metal NP and the metal film (usually the gap distance arrives in several nanometers).<sup>32,33</sup> Therefore, in the present study, we can use the scattering imaging to test our architecture. Figure 1 shows the dark-field image of many 20

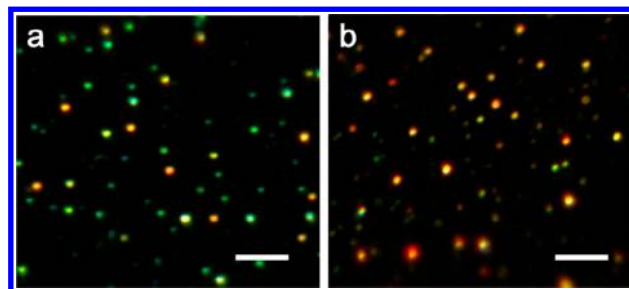


Figure 1. Dark-field images of the Ag NP-on-an-Ag film structure before (a) and after (b) the response of  $\text{Pb}^{2+}$  ions. The scale bar in (a) and (b) was 5  $\mu\text{m}$ .

nm Ag nanospheres immobilized on a 100 nm flat Ag film before (a) and after the addition of  $\text{Pb}^{2+}$  ions (b). The Ag NPs we used is 20–30 nm. After they were coated with a layer of 11-MUA (1.25 nm in length), the plasmonic band shifts to 416 nm (Supporting Information).

Most particles display green color under the dark-field illumination (Figure 1a). It should be noted that the Ag NPs were assembled on the Ag film through a ds-DNA combined with the avidin/biotin linkage. The distance of the metal NP against the metal film is about 16.02 nm in theory, involving the  $\sim 7$  nm base pair chain (calculated according to a shorter chain after the DNAzyme was hybridized with the substrate),  $\sim 6$  nm avidin, 1.52 nm 11-MUA, and  $\sim 1.5$  nm HS- $\text{C}_6$ /TEG (Supporting Information). The green scattering is mainly from the LSPR of individual spherical Ag NPs. After the DNAzyme-based plasmonic nanomechine encountered  $\text{Pb}^{2+}$  ions, the DNAzyme catalyzed a dehybridized reaction as

shown in Scheme 1 and the Ag NPs fell to the surface of the Ag film, forming a narrow gap close to 2.19 nm (the length of 11-MUA and 0.67 nm 4-ATP). It can be seen from Figure 1b that the scattering is influenced by the spacer distance and the Ag NPs started to display orange color with the distance decreasing (from 16.02 to 2.19 nm in theory), indicating the EM coupling exists between the Ag NPs and the Ag film.

Atomic force microscopy (AFM) was also used for the characterization of an Ag NP-on-an-Ag film structure before and after the addition of  $\text{Pb}^{2+}$  ions (Figure S3 in the Supporting Information). The AFM topographic images show that the mean height of AgNPs decreased after the  $\text{Pb}^{2+}$  ions were added (see the Supporting Information). The AFM results are in accordance with the dark-field characterization and prove again that our Ag NP-on-an-Ag film architecture is successful and it can response for  $\text{Pb}^{2+}$  ions by its mechanical transformation.

To achieve the quantitative and sensitive detection of lead ions, the SERS measurements of 4-ATP at different concentrations of  $\text{Pb}^{2+}$  ions were carried out. Figure 2A

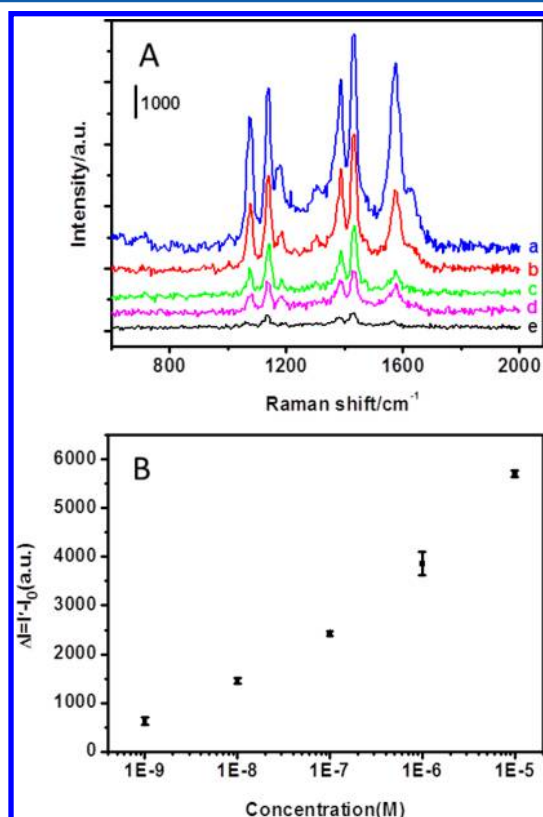


**Figure 2.** (A) SERS spectra of 4-ATP ( $1.0 \times 10^{-4}$  M) with a different concentration of  $\text{Pb}^{2+}$  ions (a)  $1.0 \times 10^{-6}$  M, (b)  $1.0 \times 10^{-7}$  M, (c)  $1.0 \times 10^{-8}$  M, (d)  $1.0 \times 10^{-9}$  M, (e) 0 M). (B) SERS intensity at  $1139 \text{ cm}^{-1}$  as a function of  $\text{Pb}^{2+}$  ion concentration. The SERS spectra were excited under the 532 nm line, approximately 29.2 mW of laser power were used to excite the sample for a signal collection time of 1 s. The error bars are calculated from three trials on the same substrate.

shows the concentration-dependent SERS spectra of 4-ATP in response for  $\text{Pb}^{2+}$  ions by the DNAzyme-based plasmonic nanomachine. We first conducted a control experiment by measuring a SERS spectrum of 4-ATP on the DNAzyme-based plasmonic nanomachine without  $\text{Pb}^{2+}$  (Figure 2A,e). It is observed that there is a very weak signal of 4-ATP (see the

assignments of the peak in Table S2 in the Supporting Information) is displayed, which is from the enhancement of the bottom bare Ag film. The Ag film in the present study was obtained by the vacuum evaporation deposition method and its thickness is 100 nm. Such a thick and almost flat Ag film has little SERS contribution.<sup>5</sup> In addition, because the Ag NP on the top end of the DNAzyme has a 16.02 nm distance from the Ag film, the coupling between them is quite weak in the local field (see Figure S4a in the Supporting Information) and the SERS contribution from the above Ag NPs can be ignored. That is also why we did not immobilize the Raman reporters (4-ATP in present study) directly on the Ag NPs like other methods in which they formed a SERS tags or labels first and then block of the metal film with BSA or others was necessary for avoiding nonspecific binding.<sup>34</sup> If the reporters are on the Ag/Au NPs, owing to the LSPR effect, a much stronger SERS signal would be obtained, which would increase the signal of the control and weaken the detection sensitivity in the present design.

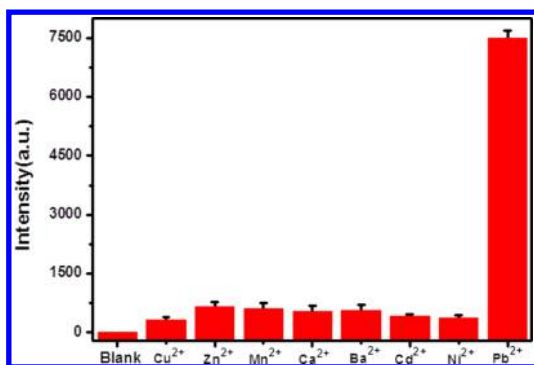
After different concentrations of  $\text{Pb}^{2+}$  were dripped on, the SERS signal intensity was obviously improved and it increased with the concentration of lead ions (Figure 2B). The enhancement in SERS signal mainly comes from the strong EM coupling in the narrower gap formed in the Ag NP-on-an-Ag film structure due to the bend of the single-stranded DNA chain. A simulated EM distribution of an Ag NP-on-an-Ag film structure with the gap distance of 2.19 nm is shown in Figure S4b in the Supporting Information. It can be observed that the electric field intensity ( $E$ ) at the gap has 300 times enhancement above the incident electric field ( $E_0$ ). Owing to the EM mechanism of SERS that SERS intensity is directly proportional to  $E^4$ ,<sup>35</sup> it can be expected that the enhancement factor of the probed signal would be  $8.1 \times 10^9$ . On the basis of this strong EM coupling, a highly sensitive detection would be expected.

Figure 2B shows the intensity of the characteristic Raman band at  $1139 \text{ cm}^{-1}$  varying with the concentration of  $\text{Pb}^{2+}$ , where  $I_0$  and  $I'$  are the SERS intensities at  $1139 \text{ cm}^{-1}$  before and after the addition of  $\text{Pb}^{2+}$  ions, and  $\Delta I$  is the actual SERS intensity of a certain concentration of Raman reporter. It can be found that the detection range is from  $1.0 \times 10^{-9}$ – $1.0 \times 10^{-5}$  M. The lowest detection concentration of  $\text{Pb}^{2+}$  by this DNAzyme-based SERS sensor is 1.0 nM while the signal-to-noise ratio is 3:1 (see the Supporting Information).

The specificity of this DNAzyme-based SERS sensor was evaluated. Interference experiments were carried out by using  $\text{Cu}^{2+}$ ,  $\text{Zn}^{2+}$ ,  $\text{Mn}^{2+}$ ,  $\text{Ca}^{2+}$ ,  $\text{Ba}^{2+}$ ,  $\text{Cd}^{2+}$ , and  $\text{Ni}^{2+}$  ( $1.0 \times 10^{-3}$  M) instead of  $\text{Pb}^{2+}$ . As is shown in Figure 3, under the same experimental conditions, the SERS intensity of the 4-ATP at the  $1139 \text{ cm}^{-1}$  did not increase significantly except for the system where  $\text{Pb}^{2+}$  was added, even though the interferences at high concentrations were employed, which suggests that this catalytic reaction exhibits good specificity toward  $\text{Pb}^{2+}$  and this simple method has a high selectivity for  $\text{Pb}^{2+}$ .

In summary, an excellent sensitive SERS sensor was fabricated to detect  $\text{Pb}^{2+}$  ions by employing a  $\text{Pb}^{2+}$  ion response DNAzyme as a spacer to construct a metallic NP-on-a film structure. The SERS reporter of 4-ATP was probed through its signal improvement that was caused by the enhanced EM field in a newborn narrower nanogap via the  $\text{Pb}^{2+}$ -induced catalytic reaction of the DNAzyme. With this smart response,  $\text{Pb}^{2+}$  ions as low as 1.0 nM can be detected, which is better than fluorescent and electrochemical





**Figure 3.** Selectivity of the DNAzyme-based SERS biosensor for Pb<sup>2+</sup> detection. The intensity of 4-ATP at 1039 cm<sup>-1</sup> for various divalent metal ions (1.0 μM for Pb<sup>2+</sup> ions and 1.0 mM for other metal ions). The error bars are from three repeat measurements on the same substrate.

sensors.<sup>36,37</sup> In a word, this DNAzyme-based SERS sensor shows characteristics of simple, efficiency, specificity, and flexibility for Pb<sup>2+</sup> detection, and it can be extended to trace other targets, e.g., amino acids,<sup>38</sup> biological small molecules,<sup>39</sup> proteins, nucleic acids,<sup>40</sup> and so on, due to the mature technology in DNA sequence programming.

## ■ ASSOCIATED CONTENT

### Supporting Information

Experimental details including materials and reagents, preparation of Ag NPs, modification of Ag NPs with 11-MUA, preparation of the lead-DNAzyme-based sensor, AFM characterization, EM field distributions of Ag NP-on-an-Ag film structures by FDTD simulation, XPS characterization of the assembly of DNAzyme and its substrate, vibrational band assignments of 4-ATP, SERS determination of Pb<sup>2+</sup> ions under 785 nm excitation, and limit of detection (LOD) of Pb<sup>2+</sup> ion determination. This material is available free of charge via the Internet at <http://pubs.acs.org>.

## ■ AUTHOR INFORMATION

### Corresponding Author

\* E-mail: [xusp@jlu.edu.cn](mailto:xusp@jlu.edu.cn).

### Notes

The authors declare no competing financial interest.

## ■ ACKNOWLEDGMENTS

This work was supported by the National Natural Science Foundation of China (Grant 21373096), National Instrumentation Program of the Ministry of Science and Technology of China Grant No. 2011YQ03012408, and the Innovation Program of the State Key Laboratory of Supramolecular Structure and Materials.

## ■ REFERENCES

- (1) Chen, C.-T.; Huang, W.-P. *J. Am. Chem. Soc.* **2002**, *124*, 6246–6247.
- (2) Chen, Y.-Y.; Chang, H.-T.; Shiang, Y.-C.; Hung, Y.-L.; Chiang, C.-K.; Huang, C.-C. *Anal. Chem.* **2009**, *81*, 9433–9439.
- (3) Kim, Y.; Johnson, R. C.; Hupp, J. T. *Nano Lett.* **2001**, *1*, 165–167.
- (4) Yuan, Y.-X.; Ling, L.; Wang, X.-Y.; Wang, M.; Gu, R.-A.; Yao, J.-L. *J. Raman Spectrosc.* **2007**, *38*, 1280–1287.
- (5) Moskovits, M. *Rev. Mod. Phys.* **1985**, *57*, 783–826.

- (6) Otto, A.; Mrozek, I.; Grabhorn, H.; Akemann, W. *J. Phys.: Condens. Matter* **1992**, *4*, 1143–1212.
- (7) Lee, C.; Wei, X.; Kysar, J. W.; Hone, J. *Science* **2008**, *321*, 385–388.
- (8) Camden, J. P.; Dieringer, J. A.; Zhao, J.; Van Duyne, R. P. *Acc. Chem. Res.* **2008**, *41*, 1653–1661.
- (9) Xu, H.; Aizpurua, J.; Käll, M.; Apell, P. *Phys. Rev. E* **2000**, *62*, 4318–4324.
- (10) Stöckle, R. M.; Suh, Y. D.; Deckert, V.; Zenobi, R. *Chem. Phys. Lett.* **2000**, *318*, 131–136.
- (11) Wang, X.; Li, M.; Meng, L.; Lin, K.; Feng, J.; Huang, T.; Yang, Z.; Ren, B. *ACS Nano* **2014**, *8*, 528–536.
- (12) Kim, N. H.; Lee, S. J.; Moskovits, M. *Nano Lett.* **2010**, *10*, 4181–4185.
- (13) Nie, S.; Emory, S. R. *Science* **1997**, *275*, 1102–1106.
- (14) Xu, H.; Bjerneld, E. J.; Käll, M.; Börjesson, L. *Phys. Rev. Lett.* **1999**, *83*, 4357–4360.
- (15) Kneipp, K.; Wang, Y.; Kneipp, H.; Perelman, L. T.; Itzkan, I.; Dasari, R. R.; Feld, M. S. *Phys. Rev. Lett.* **1997**, *78*, 1667–1670.
- (16) Tong, L.; Xu, H.; Käll, M. *MRS Bull.* **2014**, *39*, 163–168.
- (17) Halas, N. J.; Lal, S.; Chang, W.-S.; Link, S.; Nordlander, P. *Chem. Rev.* **2011**, *111*, 3913–3961.
- (18) Hatab, N. A.; Hsueh, C.-H.; Gaddis, A. L.; Retterer, S. T.; Li, J.-H.; Eres, G.; Zhang, Z.; Gu, B. *Nano Lett.* **2010**, *10*, 4952–4955.
- (19) Brousseau, L. C., III; Novak, J. P.; Marinakos, S. M.; Feldheim, D. L. *Adv. Mater.* **1999**, *11*, 447–449.
- (20) Chen, L.; Yu, Z.; Li, H.; Wang, X.; Zhao, C.; Xu, W.; Zhao, B.; Jung, Y. M. *J. Raman Spectrosc.* **2013**, *44*, 1253–1258.
- (21) Lee, J.-H.; Nam, J.-M.; Jeon, K.-S.; Lim, D.-K.; Kim, H.; Kwon, S.; Lee, H.; Suh, Y. D. *ACS Nano* **2012**, *6*, 9574–9584.
- (22) Dou, X.; Takama, T.; Yamaguchi, Y.; Yamamoto, H.; Ozaki, Y. *Anal. Chem.* **1997**, *69*, 1492–1495.
- (23) Song, S.; Wang, L.; Li, J.; Fan, C.; Zhao, J. *TrAC, Trends Anal. Chem.* **2008**, *27*, 108–117.
- (24) Wang, Y.; Irudayaraj, J. *Chem. Commun.* **2011**, *47*, 4394–4396.
- (25) Wang, H.; Kim, Y.; Liu, H.; Zhu, Z.; Bamrungsap, S.; Tan, W. J. *Am. Chem. Soc.* **2009**, *131*, 8221–8226.
- (26) Feng, D.-Q.; Liu, G.; Zheng, W.; Liu, J.; Chen, T.; Li, D. *Chem. Commun.* **2011**, *47*, 8557–8559.
- (27) Pan, T.; Uhlenbeck, O. C. *Nature* **1992**, *358*, 560–563.
- (28) Breaker, R. R.; Joyce, G. F. *Chem. Biol.* **1994**, *1*, 223–229.
- (29) Li, J.; Lu, Y. J. *Am. Chem. Soc.* **2000**, *122*, 10466–10467.
- (30) Michaels, A. M.; Nirmal, M.; Brus, L. E. *J. Am. Chem. Soc.* **1999**, *121*, 9932–9938.
- (31) Kelly, K. L.; Coronado, E.; Zhao, L. L.; Schatz, G. C. *J. Phys. Chem. B* **2003**, *107*, 668–677.
- (32) Mock, J. J.; Hill, R. T.; Degiron, A.; Zauscher, S.; Chilkoti, A.; Smith, D. R. *Nano Lett.* **2008**, *8*, 2245–2252.
- (33) Leveque, G.; Martin, O. J. F. *Opt. Express* **2006**, *14*, 9971–9981.
- (34) Ni, J.; Lipert, R. J.; Dawson, G. B.; Porter, M. D. *Anal. Chem.* **1999**, *71*, 4903–4908.
- (35) Gupta, R.; Weimer, W. A. *Chem. Phys. Lett.* **2003**, *374*, 302–306.
- (36) Li, J.; Lu, Y. J. *Am. Chem. Soc.* **2000**, *122*, 10466–10467.
- (37) Xiao, Y.; Rowe, A. A.; Plaxco, K. W. *J. Am. Chem. Soc.* **2007**, *129*, 262–263.
- (38) Roth, A.; Breaker, R. R. *Proc. Natl. Acad. Sci. U.S.A.* **1998**, *95*, 6027–6031.
- (39) Lu, L. M.; Zhang, X. B.; Kong, R. M.; Yang, B.; Tan, W. H. *J. Am. Chem. Soc.* **2011**, *133*, 11686–11691.
- (40) Zhao, X. H.; Gong, L.; Zhang, X. B.; Yang, B.; Fu, T.; Hu, R.; Tan, W. H.; Yu, R. Q. *Anal. Chem.* **2013**, *85*, 3614–3620.